COMMUNICATION

Do carbon nano-onions behave as nanoscopic Faraday cages? A comparison of the reactivity of C_{60}, C_{240}, $C_{60}@C_{240}$, $Li^+@C_{60}$, $Li^+@C_{240}$, and $Li^+@C_{60}@C_{240}$

Jesús Antonio Luque-Urrutia, Albert Poater* and Miquel Solà*

Abstract: From the analysis of the polarizability of carbon nano-onions (CNOs), it was concluded that CNOs behave as near perfect nanoscopic Faraday cages. If CNOs behave as ideal Faraday cages, the reactivity of the C_{240} cage should be the same in $Li^+@C_{240}$ and $Li^+@C_{60}@C_{240}$. In this work, we have analyzed the Diels-Alder reaction of cyclopentadiene to the free C_{240} cage and the $C_{60}@C_{240}$ CNO together with their Li^+-doped counterparts using density functional theory. We find that in all cases the preferred cycloaddition is on bond [6,6] of type B of C_{240}. Encapsulation of Li^+ results in lower enthalpy barriers due to the decrease of the energy of the LUMO orbital of the C_{240} cage. When the Li^+ is placed inside the CNO $C_{60}@C_{240}$, the decrease in enthalpy barrier is similar to that of $Li^+@C_{240}$. However, the location of Li^+ in $Li^+@C_{240}$ (off-centered) and $Li^+@C_{60}@C_{240}$ (centered) is quite different. When we place Li^+ in the center of the C_{240} cage in $Li^+@C_{240}$, the barriers increase significantly. Taking into account this effect, the barriers in $Li^+@C_{240}$ and $Li^+@C_{60}@C_{240}$ differ by about 4 kcal/mol. We attribute this result to the shielding effect of C_{60} in $Li^+@C_{60}@C_{240}$. As a result, we conclude that this CNO does not act as a perfect Faraday cage.

Carbon nano-onions (CNOs) were observed for the first time in vacuum deposited amorphous carbon films by Iijima,[1] five years before the discovery of C_{60} in 1985.[2] CNOs are spherical or polyhedral nanoparticles of carbon formed by several concentric shells of fullerenes in a structure resembling that of an onion.[3] Interestingly, CNOs have been detected in the interstellar medium.[4] Since the synthesis of CNOs by Ugarte in 1992,[5] several methods have been developed to produce them in relatively large scale.[3a, 3c, 6] Mordkovich reported in 2000, the generation of the double-shell $C_{60}@C_{240}$ and $C_{240}@C_{560}$ and triple-shell $C_{60}@C_{240}@C_{560}$ CNOs in the products of the high temperature laser pyrolysis.[7] CNOs have been recently proposed as acceptors in donor-acceptor dyads for organic photovoltaics.[8] In fact, the photoinduced lowest charge-transfer (CT) excitation in CNOs takes place at lower energy than any transition of the individual fullerenes that form the CNO.[9] Apart from its prospective use in solar cells, the number of potential applications of CNOs have grown in the last decades. Among them, we can mention their application in gas storage processes,[10] solid lubrication,[11] or heterogeneous catalysis,[12] and also as electrode materials in capacitors,[13] anode materials in lithium-ion batteries,[6a] catalyst support in fuel cells,[14] or electro-optical devices.[15] Zope et al.[16] reported in a computational study that when an external electric field is applied, the outer C_{240} or C_{180} fullerene cage almost completely shields the inner C_{60} cage in $C_{60}@C_{240}$ or $C_{60}@C_{180}$. Indeed, the polarizability of the CNOs is essentially that of the outer fullerene cage and has an insignificant contribution from the encapsulated unit. The outer fullerene cages effectively shield the encapsulated cluster and, therefore, these CNOs can be considered near perfect Faraday cages.

As in the case of fullerenes,[17] an enhancement of the applicability of CNOs (in particular, improved solubility) can be achieved through chemical functionalization. Various functionalization reactions of CNOs have been developed. The first covalent functionalized CNO was obtained in 2003 by a 1,3-dipolar addition of azomethine ylide.[18] Later on, the same reaction,[19] as well as the [2 + 1] Bingel−Hirsch cyclopropanation reaction,[20] the [2 + 1] cycloaddition of nitrenes,[21] the amidation coupling reactions[19-20] or the combination of diazonium and 1,3-dipolar additions[22] have been used to prepare a variety of CNOs derivatives.

Quite recently, ion-encapsulated fullerenes, i.e. fullerenes having an endohedral ion, have emerged as a new family of endohedral fullerenes.[23] A significant enhancement of the Diels-Alder (DA) reactivity was found for those systems having an endohedral cation. Thus, the DA reactions between cyclopenta-diene and $Li^+@C_{60}$ were reported to be significantly faster than the analogous processes involving the parent C_{60} fullerene.[24]

The effect of Li^+-encapsulated double-shell CNOs has been recently studied in CT processes.[9c] It has been found that depending on the size of the inner and outer-shells two types of CT states can be generated, namely, one with alternating charges like $Li^+@C_{60}^-@C_{240}^+$ and another with a positive charge on the outer shell as in $Li@C_{240}@C_{540}^+$. To our knowledge the effect of Li^+-encapsulated double-shell CNOs in their reactivity has not been studied yet. To fill this void, in the present work, we analyze and compare the reactivity of all different bonds of C_{60}, C_{240}, $C_{60}@C_{240}$, $Li^+@C_{60}$, $Li^+@C_{240}$, and $Li^+@C_{60}@C_{240}$ for the DA reaction with cyclopentadiene (Cp). As it is well-known, I_h-C_{60} has two different bonds, the [6,6] pyracylenic A type bond and the [5,6] corannulenic D type bond. For the studied I_h-C_{240}, one finds five different bonds (one [5,6] D type bond and four [6,6] bonds, one of them of type B and three pyrenic of type C) depicted in Figures 1 and 2. If $C_{60}@C_{240}$ behaves as a perfect Faraday cage, the effect of encapsulated Li^+ in the reactivity of the outer cage should not be affected by the inner cage. Consequently, we should have the same reactivity in $Li^+@C_{240}$ and $Li^+@C_{60}@C_{240}$. Our investigation shows that $Li^+@C_{240}$ has almost the same reactivity as $Li^+@C_{60}@C_{240}$. However, this is the result of a cancellation of effects due to the different Li^+ position in $Li^+@C_{240}$ and $Li^+@C_{60}@C_{240}$. Our results with the Li^+ placed in the center of C_{240} in $Li^+@C_{240}$ and $Li^+@C_{60}@C_{240}$ prove that $C_{60}@C_{240}$ does not behave as an ideal nanoscopic Faraday cage.

J. A. Luque-Urrutia, Dr. A. Poater, Prof. Dr. M. Solà
Institut de Química Computacional i Catàlisi (IQCC)
Facultat de Ciències, Universitat de Girona
C/ M. Aurèlia Capmany, 69, 17003 Girona, Catalonia (Spain)
E-mail: albert.poater@udg.edu; miquel.sola@udg.edu
Supporting information for this article is given via a link at the end of the document.

COMMUNICATION

The reaction profiles of the DA reaction between the different species analyzed and Cp involve first the formation of a reactant complex (RC) stabilized through van der Waals interactions that evolve to the transition state (TS) to generate the products (P). Table 1 lists the reaction enthalpy and enthalpy barriers of the DA cycloaddition of Cp to all studied species. In the case of the addition to the $[5,6]_D$ bond, there are two possible adducts that correspond to the usual *endo* and *exo* attacks in DA cycloadditions. Previous works[25] have shown that differences in these two attacks are small and, accordingly, we have analyzed only the addition that has the four carbon atoms of the cyclopentadiene most involved in the reaction facing the six-membered ring of C_{60}.

In the case of C_{60}, our calculated M06/6-31G(p,d)// PBEPBE-D3/3-21G(d) enthalpies in toluene are in good agreement with the available experimental data,[26] which show that this DA occurs exclusively over the [6,6]-bond with an activation energy of 6.9 kcal/mol (compared to our 5.4 kcal/mol for the enthalpy difference between the reactant complex and the transition state) and a reaction enthalpy of –19.8 ± 2.2 kcal/mol (compared to our –22.1 kcal/mol in Table 1). The preference for the DA to the [6,6] bond in C_{60} was attributed to the more effective <HOMO(cyclopentadiene)|LUMO(C_{60})> overlap, which is higher in the [6,6] attack along the entire reaction coordinate.[27] For the Li^+ doped C_{60} species, both the [5,6] and the [6,6] additions are faster and the reaction becomes more exothermic. In fact, the [6,6] attack becomes barrierless at this level of theory. This reactivity enhancement was found to be mainly the result of a stronger $\pi(Cp) \rightarrow \pi^*(C_{60})$ molecular orbital interaction due to the stabilization of the LUMO in cation-encapsulated fullerenes (see Table 2).[28] To our knowledge, the reactivity of icosahedral C_{240} has not been studied yet. I_h-C_{240} contains three pyrene C type [6,6] bonds that are unreactive (barriers higher than 30 kcal/mol and endothermic additions). Moreover, the corannulenic [5,6] D type bond has also a relatively large enthalpy barrier and the reaction is endothermic. Only the [6,6] bond of type B is reactive with an enthalpy barrier of 19.0 kcal/mol and a reaction enthalpy of only -2.0 kcal/mol, corresponding to a slightly exothermic cycloaddition. Not unexpectedly, the [6,6] bond of type A of C_{60} is more reactive than the [6,6] bond of type B of C_{240}. This behaviour is attributed to the higher pyramidalization angles of the C atoms in [6,6] bonds of type A than in [6,6] bonds of type B. By encapsulating Li^+ inside C_{240}, all bonds become more reactive with a reduction in the enthalpy barriers in the range of 1 to 4 kcal/mol. This is attributed to the LUMO stabilization due to the presence of the cation (Table 2). If we now compare the reactivity of C_{240} and $C_{60}@C_{240}$, we find that the two systems have almost the same reactivity, the latter being slightly more reactive (smaller enthalpy barriers) for all bonds except the $[6-6]_{C1}$. Finally, for $Li^+@C_{60}@C_{240}$, we observe the expected increase in the reactivity of the different bonds with the only exception of bond $[6-6]_{C3}$. However, the reduction in enthalpy barriers due to Li^+ is found smaller in $Li^+@C_{240}$ and $Li^+@C_{60}@C_{240}$ than in $Li^+@C_{60}$. Encapsulation of Li^+ cation lowers the enthalpy barrier of the C_{60} $[6,6]_A$, C_{240} $[6,6]_B$, and $C_{60}@C_{240}$ $[6,6]_B$ by 6.2, 1.1, and 1.7 kcal/mol, respectively. Further, it is worth noting that the enthalpy barrier of the $[6,6]_B$ attack is only 0.7 kcal/mol lower for $Li^+@C_{60}@C_{240}$ than for $Li^+@C_{240}$. This seems to indicate that $Li^+@C_{240}$ and $Li^+@C_{60}@C_{240}$ have almost the same reactivity, and, consequently, $C_{60}@C_{240}$ acts as an almost perfect Faraday cage. However, the location of Li^+ in $Li^+@C_{240}$ (off center) and $Li^+@C_{60}@C_{240}$ (center) is quite different. When we place Li^+ in the

center of the C_{240} cage in $Li^+@C_{240}$, the barriers decrease significantly by about 2-5 kcal/mol (Table 1). The reason for this reduction is that the RC is more destabilized by moving the Li^+ to the center (by 6.8 kcal/mol) than the TS (only by 2.3 kcal/mol). We attribute this effect to the fact that Li^+ interacts more favorably with the rings having the largest π charge and this charge is larger in the RC than in the TS.[29] Taking into account this effect, the barriers in $Li^+@C_{240}$ and $Li^+@C_{60}@C_{240}$ differ by about 4 kcal/mol, those of $Li^+@C_{240}$ being lower. This means that C_{60} in $Li^+@C_{60}@C_{240}$ partially shields the positive charge of the Li^+, showing that $C_{60}@C_{240}$ is not a perfect Faraday cage. This result is reinforced by two findings: first, the energy of the LUMO of $Li^+@C_{240}$ (-0.158 a.u.) is slightly smaller than that of $Li^+@C_{60}@C_{240}$ (-0.155 a.u.), indicating that the C_{60} cage has a shielding effect that reduces the reactivity of the C_{240} cage in $Li^+@C_{60}@C_{240}$; and, second, the map of electrostatic potential of $Li^+@C_{60}@C_{240}$ (Fig. S2 in the SI) shows that the electrostatic potential is similar in the inner and outer faces of C_{60} (a perfect Faraday cage should have different electrostatic potentials in the inner and outer faces).
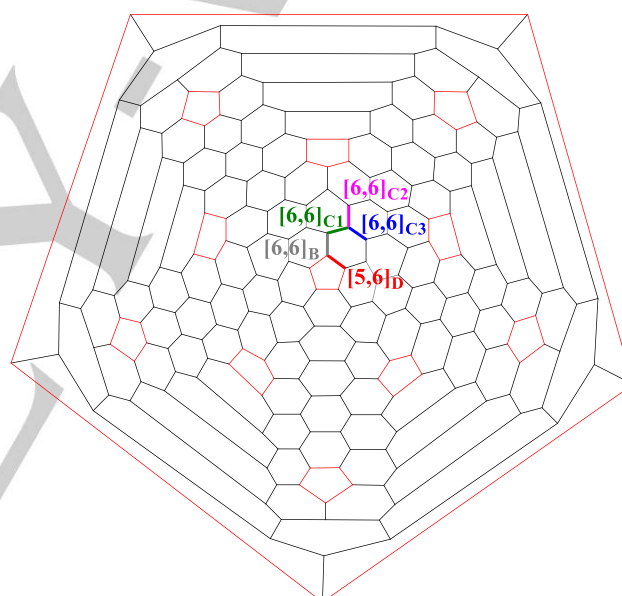

Figure 1. Schlegel diagram for a C_{240} fullerene with the five different bonds highlighted, $[5,6]_D$ in red, $[6,6]_B$ in grey, $[6,6]_{C1}$ in green, $[6,6]_{C2}$ in pink, and $[6,6]_{C3}$ in blue. The 12 pentagons of the fullerene are also marked in red.
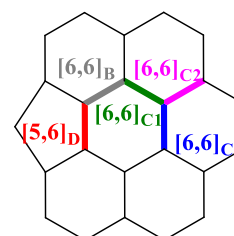

Figure 2. Representation of the different bonds found in a C_{240} cage.

Figure 3 contains the bond lengths of the two formed bonds in the RC, TS, and products of C_{240} and $C_{60}@C_{240}$ and their Li^+ doped derivatives. The data show that both C_{240} and

$C_{60}@C_{240}$ have the same bond distances. The TS is concerted but asynchronous, the bond being formed with the C atom shared with the [5,6] bond being somewhat shorter. However, when we introduce the lithium cation inside the cages, the bond lengths of the bonds being formed in the TSs are slightly elongated as expected from the Hammond postulate[30] for more exothermic reactions. Finally, the non-covalent interaction (NCI)[31] plot of the $Li^+@C_{60}@C_{240}$ displays the expected green surface between C_{60} and C_{240} as a result of the presence of attractive van der Waals interactions (see Fig. S3 in the SI).

Table 1. Reaction enthalpies (ΔH_r, enthalpy difference between adduct and reactants) and enthapies barriers ($\Delta H^\ddagger$, enthalpy difference between transition state and reactant complex) in kcal/mol of the Diels-Alder reaction between fullerenes and Cp, with toluene as solvent.

Fullerene	Bond type	$\Delta H^\ddagger$	ΔH_r
C_{60}	[5-6]$_D$	22.3	-1.9
	[6-6]$_A$	5.4	-22.1
$Li^+@C_{60}$	[5-6]$_D$	17.3	-5.8
	[6-6]$_A$	-0.8	-25.9
C_{240}	[5-6]$_D$	25.1	4.8
	[6-6]$_B$	19.0	-2.0
	[6-6]$_{C1}$	36.0	25.3
	[6-6]$_{C2}$	34.0	18.4
	[6-6]$_{C3}$	31.6	14.6
$Li^+@C_{240}$	[5-6]$_D$	21.1 (16.7)[a]	0.7 (2.2)[a]
	[6-6]$_B$	17.9 (13.4)[a]	-4.3 (-3.1)[a]
	[6-6]$_{C1}$	33.8 (31.2)[a]	23.2 (24.2)[a]
	[6-6]$_{C2}$	30.6 (28.0)[a]	18.2 (18.6)[a]
	[6-6]$_{C3}$	27.2 (23.8)[a]	9.9 (13.9)[a]
$C_{60}@C_{240}$	[5-6]$_D$	24.8	4.8
	[6-6]$_B$	18.9	-1.1
	[6-6]$_{C1}$	38.2	26.7
	[6-6]$_{C2}$	33.9	20.6
	[6-6]$_{C3}$	31.2	15.1
$Li^+@C_{60}@C_{240}$	[5-6]$_D$	22.1	1.7
	[6-6]$_B$	17.2	-3.8
	[6-6]$_{C1}$	35.1	23.6
	[6-6]$_{C2}$	33.9	16.1
	[6-6]$_{C3}$	33.2	12.1

[a] Enthalpies in parentheses are from single point calculations with the Li^+ placed in the center of the C_{240} cage. Thermal corrections were taken from the PBEPBE-D3/3-21G(d) optimized systems.

Table 2. Energy of the LUMO for the different fullerenes studied in this work.

Reactant	LUMO (a.u.)
C_{60}	-0.114
$Li^+@C_{60}$[a]	-0.179
C_{240}	-0.124
$Li^+@C_{240}$	-0.158
$C_{60}@C_{240}$	-0.124
$Li^+@C_{60}@C_{240}$[b]	-0.155

[a] For $Li^+@C_{60}$, we report the energy of LUMO +1 (LUMO is located on the Li cation). [b] For $Li^+@C_{60}@C_{240}$, we provide the energy of the LUMO +5 (LUMO is located in the Li cation and the LUMO +1,+2,+3,+4 orbitals are located on the C_{60} cage).

In conclusion, we have studied the reactivity of the different bonds for the DA reaction of cyclopentadiene to C_{60}, C_{240}, and $C_{60}@C_{240}$ as well as their Li^+-doped counterparts. In all species the preferred attack is on bond [6,6] either of type A (for C_{60} cages) or type B (for C_{240} cages). The most favored attack in C_{240} is slightly exothermic, the rest being endothermic. Encapsulation of Li^+ results in a decrease of the energy of the LUMO orbital of the outer cage that results in lower enthalpy

barriers for all attacks. When the Li^+ is placed inside the CNO $C_{60}@C_{240}$, the decrease is smaller. We attribute this result to the shielding effect of C_{60}. Since no shielding is expected in a perfect Faraday cage, we conclude that this CNO does not act as an ideal Faraday cage.
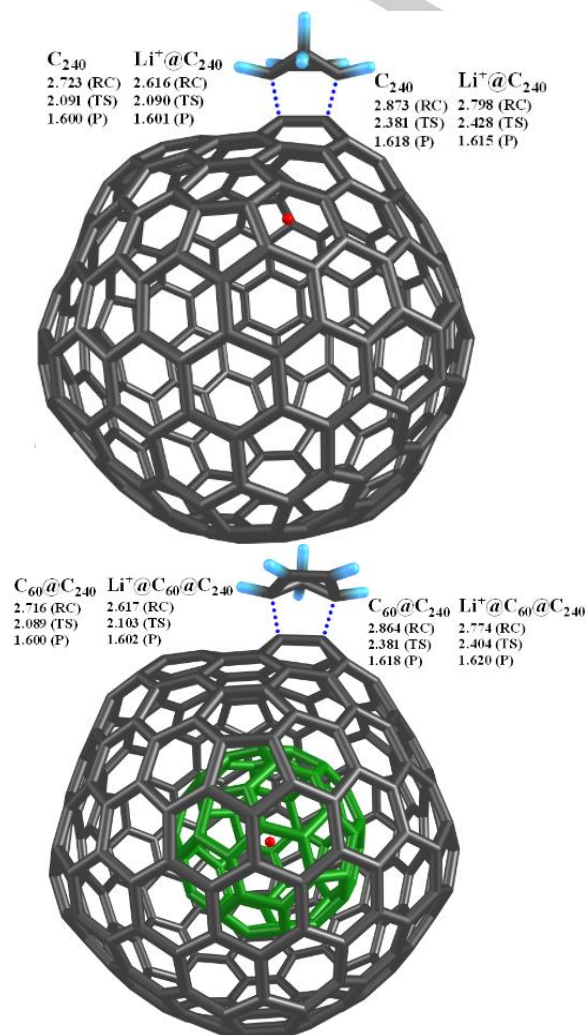

Figure 3. Bond distances (in Å) of the two new bonds being formed in the reactant complex (RC), transition state (TS), and product (P) for C_{240} and $Li^+@C_{240}$ (top) and for $C_{60}@C_{240}$ and $Li^+@C_{60}@C_{240}$ (bottom) for the most reactive [6,6]$_B$ bond. Inner fullerene colored in green for the sake of clarity. Li^+ is represented as a red dot.

Computational details

All density functional theory calculations were performed with the Gaussian16 set of programs.[32] A benchmark of different functionals and basis sets was done for the DA to C_{60} and the results were compared to experimental data (see Table S1 in the SI). The electronic configuration of the molecular systems was described with the pure functional of Perdew, Burke, and Ernzerhof (PBEPBE keyword in Gaussian16) using the small split-valence basis set 3-21G(d)[33] due to the size of the target species (Fig. S1 of the SI shows that the geometries obtained with a larger basis set such as the 6-311G(d,p) are almost indistinguishable from those obtained with the 3-21G(d) basis set). Since corrections due to dispersion are essential to study the reactivity in carbon nanostructures,[34] we have included them

through the Grimme's method with Becke-Johnson damping[35] (GD3BJ keyword in Gaussian). The geometry optimizations were performed without symmetry constraints and the characterization of the local stationary points was carried out by analytical frequency calculations. These frequencies were used to calculate unscaled zero-point energies (ZPEs) as well as thermal corrections and entropy effects at 298.15 K and 1 atm. We obtained the energies by single-point calculations on the optimized geometries with the M06 functional[36] and the double-zeta polarized basis set 6-31G(d,p)[37] for increased accuracy. Solvent effects were included with the polarizable continuous solvation model (PCM)[38] using toluene as a solvent. The reported enthalpies in this work are electronic energies obtained at the M06/6-31G(d,p)//PBEPBE-D3/3-21G(d) level of theory corrected with zero-point energies, thermal corrections and entropy effects evaluated at 298.15 K and 1 atm.

Supporting Information

Cartesian coordinates of all optimized species, benchmark calculations, electrostatic map, and noncovalent interactions plot.

References

[1]   S. Iijima, *J. Cryst. Growth* **1980**, *50*, 675-683.
[2]   H. W. Kroto, J. R. Heath, S. C. O'Brien, R. F. Curl, R. E. Smalley, *Nature* **1985**, *318*, 162-163.
[3]   [a] B.-s. Xu, *New Carbon Mater.* **2008**, *23*, 289-301; [b] L. Echegoyen, A. L. Ortiz, M. N. Chaur, A. J. Palkar, in *Chemistry of Nanocarbons* (Eds.: T. Akasaka, F. Wudl, S. Nagase), John Wiley & Sons, Chichester, **2010**; [c] J. Bartelmess, S. Giordani, *Beilstein J. Nanotechnol.* **2014**, *5*, 1980-1998.
[4]   [a] W. A. de Heer, D. Ugarte, *Chem. Phys. Lett.* **1993**, *207*, 480-486; [b] S. Iglesias-Groth, *Astrophys. J.* **2004**, *608*, L37-L40.
[5]   D. Ugarte, *Nature* **1992**, *359*, 707-709.
[6]   [a] F.-D. Han, B. Yao, Y.-J. Bai, *J. Phys. Chem. C* **2011**, *115*, 8923-8927; [b] V. Z. Mordkovich, Y. Shiratori, H. Hiraoka, Y. Takeuchi, *Phys. Solid State* **2002**, *44*, 603-606.
[7]   V. Z. Mordkovich, *Chem. Mater.* **2000**, *12*, 2813-2818.
[8]   D. M. Bobrowska, H. Zubyk, E. Regulska, E. Romero, L. Echegoyen, M. E. Plonska-Brzezinska, *Nano Adv.* **2019**, *1*, 3164-3176.
[9]   [a] A. A. Voityuk, M. Solà, *J. Phys. Chem. A* **2016**, *120*, 5798-5804; [b] M. A. Hashmi, M. Lein, *J. Phys. Chem. C* **2018**, *122*, 2422-2431; [c] A. J. Stasyuk, O. A. Stasyuk, M. Solà, A. A. Voityuk, *J. Phys. Chem. C* **2019**, *123*, 16525-16532.
[10]   N. Sano, H. Wang, I. Alexandrou, M. Chhowalla, K. B. K. Teo, G. A. J. Amaratunga, K. Iimura, *J. App. Phys.* **2002**, *92*, 2783-2788.
[11]   A. Hirata, M. Igarashi, T. Kaito, *Tribol. Int.* **2004**, *37*, 899-905.
[12]   N. Keller, N. I. Maksimova, V. V. Roddatis, M. Schur, G. Mestl, Y. V. Butenko, V. L. Kuznetsov, R. Schlögl, *Angew. Chem. Int. Ed.* **2002**, *41*, 1885-1888.
[13]   D. Pech, M. Brunet, H. Durou, P. Huang, V. Mochalin, Y. Gogotsi, P.-L. Taberna, P. Simon, *Nat. Nanotechnol.* **2010**, *5*, 651-654.
[14]   B. Xu, X. Yang, X. Wang, J. Guo, X. Liu, *J. Power Sources* **2006**, *162*, 160-164.
[15]   E. Koudoumas, O. Kokkinaki, M. Konstantaki, S. Couris, S. Korovin, P. Detkov, V. Kuznetsov, S. Pimenov, V. Pustovoi, *Chem. Phys. Lett.* **2002**, *357*, 336-340.
[16]   [a] R. R. Zope, *J. Phys. B: At. Mol. Opt. Phys.* **2008**, *41*, 085101; [b] R. R. Zope, S. Bhusal, L. Basurto, T. Baruah, K. Jackson, *J. Chem. Phys.* **2015**, *143*, 084306.
[17]   [a] A. Hirsch, *The Chemistry of Fullerenes*, Thieme, Sttutgart, Germany, **1994**; [b] A. Hirsch, M. Brettreich, Weinheim, **2004**.
[18]   V. Georgakilas, D. M. Guldi, R. Signorini, R. Bozio, M. Prato, *J. Am. Chem. Soc.* **2003**, *125*, 14268-14269.
[19]   A. S. Rettenbacher, B. Elliott, J. S. Hudson, A. Amirkhanian, L. Echegoyen, *Chem. Eur. J.* **2006**, *12*, 376-387.
[20]   A. Palkar, F. Melin, C. M. Cardona, B. Elliott, A. K. Naskar, D. D. Edie, A. Kumbhar, L. Echegoyen, *Chem. Asian J.* **2007**, *2*, 625-633.
[21]   L. Zhou, C. Gao, D. Zhu, W. Xu, F. F. Chen, A. Palkar, L. Echegoyen, E. S.-W. Kong, *Chem. Eur. J.* **2009**, *15*, 1389-1396.
[22]   K. Flavin, M. N. Chaur, L. Echegoyen, S. Giordani, *Org. Lett.* **2010**, *12*, 840-843.
[23]   [a] S. Aoyagi, E. Nishibori, H. Sawa, K. Sugimoto, M. Takata, Y. Miyata, R. Kitaura, H. Shinohara, H. Okada, T. Sakai, Y. Ono, K. Kawachi, K. Yokoo, S. Ono, K. Omote, Y. Kasama, S. Ishikawa, T. Komuro, H. Tobita, *Nature Chem.* **2010**, *2*, 678-683; [b] S. Fukuzumi, K. Ohkubo, Y. Kawashima, D. S. Kim, J. S. Park, A. Jana, V. M. Lynch, D. Kim, J. L. Sessler, *J. Am. Chem. Soc.* **2011**, *133*, 15938-15941; [c] S. Aoyagi, Y. Sado, E. Nishibori, H. Sawa, H. Okada, H. Tobita, Y. Kasama, R. Kitaura, H. Shinohara, *Angew. Chem. Int. Ed.* **2012**, *51*, 3377-3381; [d] H. Ueno, K. Kokubo, Y. Nakamura, K. Ohkubo, N. Ikuma, H. Moriyama, S. Fukuzumi, T. Oshima, *Chem. Commun.* **2013**, *49*, 7376-7378.
[24]   [a] H. Kawakami, H. Okada, Y. Matsuo, *Org. Lett.* **2013**, *15*, 4466-4469; [b] H. Ueno, H. Kawakami, K. Nakagawa, H. Okada, N. Ikuma, S. Aoyagi, K. Kokubo, Y. Matsuo, T. Oshima, *J. Am. Chem. Soc.* **2014**, *136*, 11162-11167.
[25]   [a] M. Solà, J. Mestres, J. Martí, M. Duran, *Chem. Phys. Lett.* **1994**, *231*, 325-330; [b] M. Cases, M. Duran, J. Mestres, N. Martín, M. Solà, in *Fullerenes for the New Millennium, Vol. 11* (Eds.: P. V. Kamat, D. M. Guldi, K. M. Kadish), **2001**, pp. 244-269.
[26]   [a] L. M. Giovane, J. W. Barco, T. Yadav, A. L. Lafleur, J. A. Marr, J. B. Howard, V. M. Rotello, *J. Phys. Chem.* **1993**, *97*, 8560-8561; [b] L. S. K. Pang, M. A. Wilson, *J. Phys. Chem.* **1993**, *97*, 6761-6763.
[27]   I. Fernández, M. Solà, F. M. Bickelhaupt, *Chem. Eur. J.* **2013**, *19*, 7416-7422.
[28]   Y. García-Rodeja, M. Solà, F. M. Bickelhaupt, I. Fernández, *Chem. Eur. J.* **2017**, *23*, 11030-11036.
[29]   M. Güell, J. Poater, J. M. Luis, O. Mó, M. Yáñez, M. Solà, *ChemPhysChem* **2005**, *6*, 2552-2561.
[30]   G. S. Hammond, *J. Am. Chem. Soc.* **1955**, *77*, 334-338.
[31]   J. Contreras-García, E. R. Johnson, S. Keinan, R. Chaudret, J.-P. Piquemal, D. N. Beratan, W. Yang, *J. Chem. Theory Comput.* **2011**, *7*, 625-632.
[32]   M. J. Frisch et al., Gaussian 16, rev. B.01, Wallingford, CT, **2016**.
[33]   [a] J. S. Binkley, J. A. Pople, W. J. Hehre, *J. Am. Chem. Soc.* **1980**, *102*, 939-947; [b] M. S. Gordon, J. S. Binkley, J. A. Pople, W. J. Pietro, W. J. Hehre, *J. Am. Chem. Soc.* **1982**, *104*, 2797-2803.
[34]   S. Osuna, M. Swart, M. Solà, *J. Phys. Chem. A* **2011**, *115*, 3491-3496.
[35]   [a] S. Grimme, S. Ehrlich, L. Goerigk, *J. Comput. Chem.* **2011**, *32*, 1456-1465; [b] A. D. Becke, E. R. Johnson, *J. Chem. Phys.* **2005**, *122*, 154104.
[36]   Y. Zhao, D. G. Truhlar, *Theor. Chem. Acc.* **2008**, *120*, 215-241.
[37]   [a] R. Ditchfield, W. J. Hehre, J. A. Pople, *J. Chem. Phys.* **1971**, *54*, 724-728; [b] W. J. Hehre, R. Ditchfield, J. A. Pople, *J. Chem. Phys.* **1972**, *56*, 2257-2261.
[38]   [a] G. Scalmani, M. J. Frisch, *J. Chem. Phys.* **2010**, *132*, 114110; [b] J. Tomasi, B. Mennucci, R. Cammi, *Chem. Rev.* **2005**, *105*, 2999-3094.

Graphic for TOC
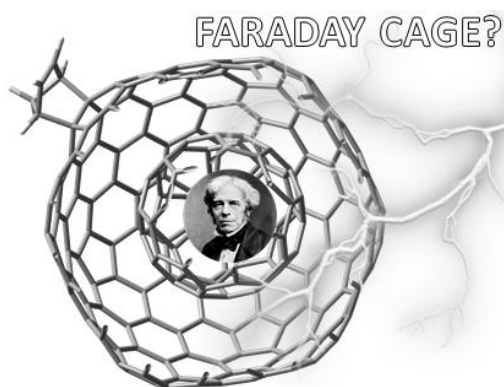
FARADAY CAGE?

The comparison of the chemical reactivity of $Li^+@C_{240}$ and $Li^+@C_{60}@C_{240}$ indicates that $C_{60}@C_{240}$ does not act as an ideal Faraday cage.